REVISTAMATĒRIA V.31
ISSN 1517-7076 articles e20260162, 2026

Mechanical performance optimization of concrete incorporating Crushed Brick Aggregates and manufactured sand using Response Surface Methodology

Arivumani Vaiyapuri[1], Kousalyadevi Gopu[2],
Shoba Kannaiyan Balakrishnan[3], Priyadharsini Karthikeyan[4]

[1]Meenakshi College of Engineering, School of Architecture. Chennai, Tamil Nadu, India.
[2]Mepco Schlenk Engineering College, Department of Civil Engineering. Sivakasi, Tamil Nadu, India.
[3]St. Peter's College of Engineering and Technology, School of Architecture. Chennai, Tamil Nadu, India.
[4]Tagore Engineering College, Department of Physics. Chennai, Tamil Nadu, India.
e-mail: arivumaniv7@gmail.com, kousym.arch@gmail.com, haridrab002@gmail.com, tecpriyaphy@gmail.com

ABSTRACT

The transition toward sustainable construction necessitates the strategic reuse of demolition waste as a substitute for virgin aggregates. While environmental and economic benefits are clear, the challenge lies in the inferior mechanical properties typical of recycled materials compared to natural stone. This research addresses these limitations by exploring the synergy between Crushed Brick Aggregates (CBA) and Manufactured Sand (M-Sand). By optimizing these components, the study encourages denser matrix formation and improved interfacial bonding. The objective is to engineer a moderate-strength composite that balances environmental goals with structural requirements. Fresh and hardened state characterizations, specifically workability, density, and mechanical strengths, were conducted to assess the performance of the proposed concrete. The roles of CBA and M-Sand were scrutinized via experimental protocols and enhanced through statistical modelling. Mix optimization was achieved using RSM and CCD, with model reliability confirmed through ANOVA. The interaction of variables was graphically represented in 3D response surface plots, leading to the conclusion that a 40% CBA and 60% M-Sand configuration is optimal for cost-effectiveness and sustainability. Microstructural validation through thin-section analysis evidenced a robust aggregate–matrix bond, corroborating the measured mechanical improvements.

Keywords: Manufactured Sand (M-Sand); Recycled construction waste; Response Surface Methodology; Sustainable development; Demolition waste.

1. INTRODUCTION

Concrete remains the most extensively used construction material worldwide due to its versatility, durability, and cost-effectiveness across a wide range of structural and infrastructural applications. Its indispensability to modern construction has resulted in unprecedented demand, which has, in turn, intensified concerns regarding resource depletion and environmental sustainability. Among the constituent materials of concrete, aggregates constitute approximately 60–75% of the total volume and exert a dominant influence on its mechanical properties, including compressive strength, tensile capacity, and flexural performance [1, 2]. Consequently, any modification to the aggregate phase has a direct and significant impact on the overall behaviour of concrete. The continuous extraction of natural aggregates has led to severe ecological consequences, such as riverbed depletion, quarry-induced landscape degradation, biodiversity loss, and increased greenhouse gas emissions associated with material processing and transportation [3, 4]. These challenges necessitate the exploration of alternative aggregate materials capable of enhancing mechanical performance while reducing environmental burdens. The construction industry is one of the most resource-intensive sectors globally, accounting for nearly 50% of total raw material consumption, approximately 40% of energy usage, and close to 50% of solid waste generation [5, 6]. These alarming figures have prompted increased emphasis on sustainable construction practices based on circular economy principles, which advocate the reuse of waste materials and a reduction in dependence on virgin resources [7]. Within this framework, the incorporation of construction and demolition waste into concrete

Corresponding Author: Arivumani Vaiyapuri Received on 21/02/2026 Accepted on 06/05/2026

DOI: https://doi.org/10.1590/1517-7076-RMAT-2026-0162

production has emerged as a promising strategy for improving sustainability without compromising structural integrity. Brick and ceramic wastes constitute a significant fraction of construction and demolition debris, particularly in rapidly urbanizing regions. Large quantities of rejected bricks, masonry rubble, and ceramic fragments are generated from manufacturing defects, demolition activities, and renovation projects. These wastes are commonly disposed of in landfills, where they occupy valuable land resources and pose long-term environmental risks, including dust pollution, surface runoff contamination, and the leaching of alkaline compounds into soil and groundwater systems [8, 9]. Diverting brick waste from landfills into concrete production offers a sustainable waste management solution while providing an alternative source of aggregates. Crushed Brick Aggregates (CBA), derived from discarded or demolished clay bricks, have received increasing research attention as substitutes for natural coarse aggregates. Brick materials are predominantly composed of silica and alumina, contributing to their chemical stability and compatibility with cementitious matrices [10]. Several studies have demonstrated that concrete incorporating CBA can achieve compressive strength comparable to that of conventional concrete when used within optimized replacement limits [11]. Additionally, the rough surface texture and angular shape of brick aggregates enhance mechanical interlocking and improve the bond between the aggregate and cement paste [12]. However, the relatively higher porosity and water absorption of CBA may adversely affect workability and early-age strength development if not properly accounted for during mix design [13]. These characteristics highlight the need for systematic optimization to maximize the mechanical benefits of CBA in concrete. In parallel with coarse aggregate substitution, the depletion of natural river sand has become a critical issue in concrete production. Excessive sand mining has resulted in riverbank erosion, lowering of groundwater tables, and disruption of aquatic ecosystems, leading to strict regulatory restrictions in many regions [14]. Manufactured Sand (M-Sand), produced through controlled crushing and grading processes, has therefore gained recognition as a viable alternative to natural sand. M-Sand offers advantages such as consistent particle size distribution, reduced impurities, and angular particle morphology, which can enhance packing density and improve interfacial transition zone (ITZ) characteristics when properly incorporated into concrete mixtures [15]. Brick waste provides a viable and underutilized source material for the production of Manufactured Sand. Fine particles obtained from crushing brick waste can be processed to meet standard grading requirements for fine aggregates. Brick-derived M-Sand exhibits angularity and a rough surface texture, promoting mechanical interlocking and improving bonding with cement paste [16]. These features can enhance compressive, split tensile, and flexural strengths when appropriate replacement levels are used. However, excessive incorporation of brick-based M-Sand may increase water demand and reduce workability due to its angular nature and higher fines content [17]. Therefore, optimizing the proportion of brick-derived M-Sand is essential to achieve a balance between fresh and hardened concrete properties. Although numerous studies have investigated the individual effects of Crushed Brick Aggregates and Manufactured Sand on concrete performance, limited research has examined their combined influence on mechanical properties. The interaction between coarse aggregate replacement with CBA and fine aggregate substitution using brick-derived M-Sand introduces complex interdependencies that cannot be effectively captured through conventional trial-and-error mix design methods. Such traditional approaches are time-consuming, material-intensive, and often fail to identify optimal combinations of multiple influencing variables. In this context, Response Surface Methodology (RSM) has emerged as a robust statistical and mathematical tool for modelling, analysing, and optimizing multivariable systems [18]. RSM enables the evaluation of both individual and interaction effects of input parameters on selected response variables while significantly reducing the number of experimental trials required. Its application in concrete technology has proven effective for optimizing mix proportions, predicting mechanical performance, and identifying optimal replacement thresholds for sustainable materials [19]. By employing RSM, it is possible to systematically explore the combined effects of CBA and Manufactured Sand on concrete strength characteristics and identify optimal mix configurations. The present study adopts an RSM-based approach to enhance the mechanical properties of concrete incorporating Crushed Brick Aggregates as coarse aggregates and brick-derived Manufactured Sand as fine aggregates. The primary objective is to determine optimal replacement levels that maximize compressive strength, split tensile strength, and flexural strength while maintaining acceptable workability and structural performance. These mechanical properties are selected as key response variables due to their critical importance in structural design and serviceability. In addition to mechanical testing, microstructural investigations using thin-section microscopy are conducted to elucidate the relationship between aggregate morphology, ITZ development, and observed strength behaviour [20]. The findings of this research demonstrate that optimized combinations of CBA and brick-based M-Sand can significantly enhance the mechanical properties of concrete compared to conventional mixes. Moderate replacement levels lead to improved strength performance due to enhanced particle packing and improved aggregate–paste bonding, whereas excessive substitution results in reduced workability and strength loss. By integrating recycled brick aggregates within a statistically optimized RSM framework, this study provides a comprehensive and performance-oriented approach for the development of sustainable concrete. The outcomes contribute to the advancement of circular construction practices and offer practical guidance for the large-scale application of recycled brick aggregates and Manufactured Sand in structural concrete. Previous studies indicate that aggregates reclaimed from demolished structures contain a combination of lithic materials and residual cementitious mortar, resulting in diminished mechanical properties. This degradation is intrinsically linked to the characteristics of the interfacial transition zone and the geometric arrangement of aggregate particles. To ensure compliance with structural requirements, adherence to national durability protocols—particularly the control of the water-to-binder (w/b) ratio—is essential [21]. Innovative mixing strategies incorporating pozzolanic materials have also been shown to enhance carbonation processes and improve composite performance [22]. These methodologies provide a framework for analysing Crushed Brick Aggregates (CBA) and Manufactured Sand (M-Sand) in sustainable concrete design. Existing literature further highlights the pozzolanic activity of fine ceramic materials, noting their ability to enhance mechanical performance through the formation of additional calcium silicate hydrate (C–S–H) gel [23]. In alignment with sustainable engineering practices, the present study utilizes Crushed Brick Aggregate (CBA) and Manufactured Sand (M-Sand) as coarse and fine aggregate replacements, respectively. This investigation focuses on the development of a medium-strength, eco-friendly composite suitable for sustainable structural applications. A standardized two-stage mixing procedure [24] was employed to evaluate the fresh and hardened performance of various CBA and M-Sand combinations, with particular emphasis on compressive, flexural, and split tensile strengths. Optimization was achieved through the application of Response Surface Methodology (RSM), which provides a robust mathematical and statistical framework for analysing experimental data. This approach enables visualization of interactions among variables and minimizes redundant experimental trials while identifying optimal mixture proportions [25, 26]. Despite extensive studies on either Crushed Brick Aggregates or Manufactured Sand individually, limited research has systematically investigated their combined use in concrete and the resulting interaction effects on fresh and hardened properties. In particular, there is a lack of robust optimization-based studies integrating RSM with microstructural validation to determine optimal replacement levels for achieving balanced mechanical performance and sustainability.

2. MATERIALS AND METHODS

2.1. Materials

2.1.1. Crushed brick aggregates

The Crushed Brick Aggregate (CBA) was procured from a demolition site, characterized by the adhesion of aged mortar to the original aggregate surfaces. CBA is distinguished by its porous and lightweight mortar phase, which contributes to a reduced specific gravity and density relative to virgin aggregates. The mineralogical profile of the CBA was established through X-ray Diffraction (XRD) analysis. The experimental results are graphically represented in Figure 1 and tabulated for reference in Table 1.

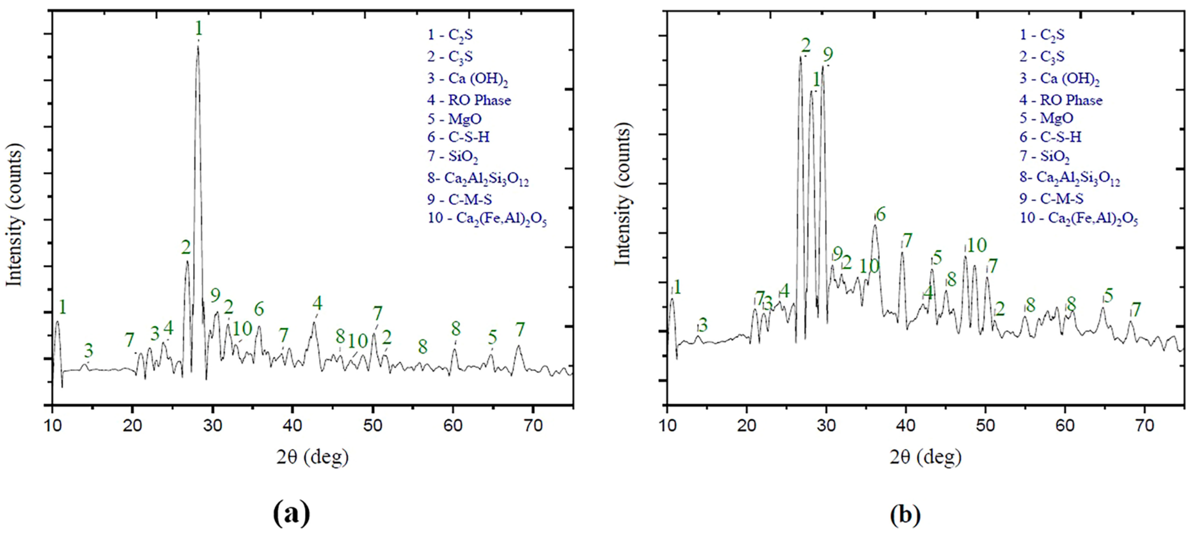

Figure 1: X-ray Diffraction analysis of M-sand and CBA.

2.1.2. Recycled brick waste

The raw material constituents of brick waste, feldspar, kaolin, and bone ash, significantly influence the chemical profile of the secondary M-Sand. The presence of kaolin, a hydrated aluminum silicate, ensures a high concentration of silicon and aluminum oxides within the composite. The mineralogical identification of the M-Sand was performed using X-ray diffraction, the results of which are depicted in Figure 1, with additional property data provided in Table 1.

2.2. Sample selection and preparation

The preparation of recycled materials involved initial washing to eliminate impurities from the CBA. Mechanical reduction was performed via jaw crushers to produce coarse and fine fractions, targeting a maximum size of 20 mm for CBA and 4.75 mm for M-Sand. Following the requirements of BIS 383 [26], the M-Sand was graded to ensure its suitability for concrete production [27]. Figure 2 provides the particle size distribution plots, illustrating the sieve analysis results for both aggregate types.

2.3. Mixing technique and mix composition

This research implemented the dual-stage blending strategy developed by TAM *et al.* [24], a technique specifically engineered to optimize the performance of concrete containing recycled aggregates. In the initial stage, a cement paste was prepared by combining water, cement, and supplementary components; the CBA was then gradually incorporated and mixed continuously for 10 minutes. The second stage involved the addition of natural coarse particles and M-Sand to complete the matrix. This approach is designed to enhance the interfacial bond of recycled materials. Following IS 10262:2019 standards for an M30 grade mix design [28], sixteen distinct combinations were formulated with a constant w/b ratio of 0.45 as shown in Table 2. Both CBA and M-Sand served as substitutes for coarse and fine aggregates, respectively, at replacement levels ranging from 0% to 100% in 20% increments.

Table 1: Characteristics of M-Sand and CBA.

CHARACTERISTICS	M-SAND	CBA
Maximum aggregate size	4.75 mm	20 mm
Fineness modulus	3.08	6.42
Grading zone	Zone 2	–
Specific gravity	2.25	3.14
Water absorption	2.9%	1.6%

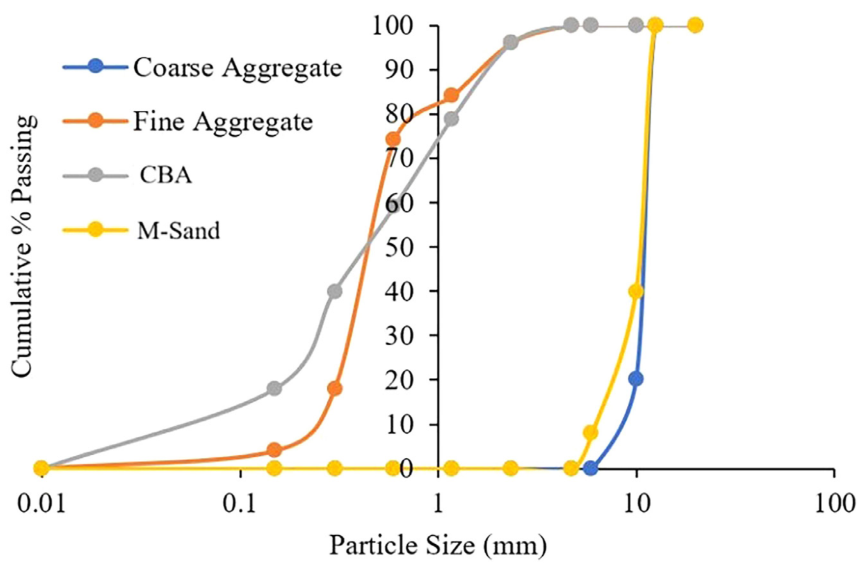

Figure 2: Various aggregates particle size distribution curve.

Table 2: Mix ratios.

MIX	CEMENT IN kg/m³	NATURAL SAND IN kg/m³	M-SAND POWDER IN kg/m³	CA IN kg/m³	CBA IN kg/m³
B0-R0	494	840	0	1185	0
B20-R0		672	168	1185	0
B40-R0		504	336	1185	0
B60-R0		336	504	1185	0
B80-R0		168	672	1185	0
B100-R0		0	840	1185	0
B0-R20		840	0	948	237
B0-R40		840	0	711	474
B0-R60		840	0	474	711
B0-R80		840	0	237	948
B0-R100		840	0	0	1185
B40-R40		504	336	711	474
B40-R60		504	336	474	711
B60-R40		336	504	711	474
B60-R60		336	504	474	711
B100-R100		0	840	0	1185

2.4. Experiment design

In this study, the experimental program was systematically designed using Response Surface Methodology (RSM) based on a Central Composite Design (CCD) to investigate the combined effects of Manufactured Sand (M-Sand) and Crushed Brick Aggregates (CBA) on the fresh and hardened properties of concrete. Two independent variables were considered, namely M-Sand replacement level (A) and CBA replacement level (B), each varied at five coded levels (−α, −1, 0, +1, +α) to capture linear, interaction, and quadratic effects within the experimental domain. The CCD framework comprised factorial points, axial (star) points, and center points, enabling the development of second-order polynomial regression models while ensuring reliable estimation of experimental error and model curvature. Three specimens (n = 3) were cast for each mix proportion to ensure repeatability, statistical reliability, and consistency of results. Compressive strength was determined using 150 × 150 × 150 mm cube specimens in accordance with IS 516 (Part 1): 2021 and ASTM C39, split tensile strength was evaluated using 150 × 300 mm cylindrical specimens as per IS 5816: 1999 and ASTM C496, and flexural strength was assessed using 100 × 100 × 500 mm beam specimens following IS 516 (Part 1): 2021 and ASTM C78. After casting, all specimens were demoulded after 24 hours and cured in water tanks maintained at a controlled temperature of 27 ± 2 °C and relative humidity of approximately 95 ± 2%, ensuring uniform hydration conditions for all mixes. Curing was carried out consistently until the specified testing ages of 7 and 28 days. The experimental responses were analysed using Analysis of Variance (ANOVA) to evaluate the significance of model terms, interaction effects, and overall model fitness at a 95% confidence level. Model adequacy was assessed using the coefficient of determination (R^2), adjusted R^2, F-value, lack-of-fit test, and p-value. Regression models were developed using coded variables to improve numerical stability and allow direct comparison of factor effects, while actual percentage values were used during batching and mix preparation. The transformation between coded and actual variables followed standard RSM normalization procedures. Additionally, three-dimensional response surface plots and contour diagrams were generated to visually interpret interaction effects between variables and to identify optimal replacement levels for enhanced mechanical performance and sustainable concrete development.

3. RESULTS AND DISCUSSION

The characterization of the various design mixes is presented in Table 3, encompassing an assessment of their properties in the fresh and hardened phases. This analysis is specifically directed toward the evaluation of

Table 3: Investigational outcomes.

MIX	SLUMP (mm)	Δ SLUMP (%)	DENSITY (kg/m³)	Δ DENSITY (%)	CS (MPa)	Δ CS (%)	STS (MPa)	Δ STS (%)	FS (MPa)	Δ FS (%)
B0–R0	71	0.00	2369	0.00	35.98	0.00	3.69	0.00	4.12	0.00
B20–R0	63	–11.27	2357	–0.51	37.28	+3.61	3.88	+5.15	4.37	+6.07
B40–R0	53	–25.35	2358	–0.46	41.69	+15.85	4.17	+12.97	4.68	+13.59
B60–R0	46	–35.21	2319	–2.11	43.07	+19.69	4.19	+13.55	4.76	+15.53
B80–R0	43	–39.44	2309	–2.54	40.38	+12.19	4.37	+18.43	4.69	+13.83
B100–R0	34	–52.11	2289	–3.38	39.02	+8.43	4.54	+23.03	4.43	+7.52
B0–R20	68	–4.23	2358	–0.46	36.79	+2.25	3.78	+2.44	4.27	+3.64
B0–R40	61	–14.08	2322	–1.98	39.21	+9.00	3.89	+5.42	4.38	+6.31
B0–R60	58	–18.31	2307	–2.62	39.89	+10.89	4.09	+10.84	4.49	+8.98
B0–R80	47	–33.80	2282	–3.67	36.38	+1.11	3.58	–2.98	4.17	+1.21
B0–R100	41	–42.25	2268	–4.26	33.29	–7.50	3.37	–8.67	4.02	–2.43
B40–R40	42	–40.85	2327	–1.77	39.47	+9.70	4.06	+10.03	4.59	+11.41
B40–R60	40	–43.66	2307	–2.62	36.38	+1.11	3.87	+4.88	4.38	+6.31
B60–R40	33	–53.52	2319	–2.11	41.28	+14.48	4.19	+13.55	4.71	+14.32
B60–R60	27	–61.97	2295	–3.13	38.02	+5.68	4.01	+8.67	4.48	+8.74
B100–R100	25	–64.79	2262	–4.51	33.49	–6.92	3.52	–4.61	4.09	–0.73

mechanical efficacy, as evidenced by the compressive, flexural, and split tensile strength measurements recorded for the formulated CBA and M-Sand composites.

3.1. Workability analysis

The slump value of concrete is a critical indicator of its uniformity, flowability, compaction, and pumpability. Investigations into the effects of M-Sand and CBA on concrete workability reveal that workability typically diminishes as replacement ratios increase, primarily due to the higher water absorption rates of these recycled materials. For construction engineers, the ability to forecast workability accurately is essential for field applications. A regression analysis was conducted to predict slump values for specific percentages of M-Sand (x) and CBA (y). Table 4 details the ANOVA results and the corresponding regression equations modelling workability (w) in mm.

$$w = 71.5625 - 0.38\ x - 0.2875\ y + 0.0021\ xy \tag{1}$$

Statistical validation of the workability model yielded a coefficient of determination (R^2) of 0.9909 and an adjusted $R^2$of 0.9886, indicating superior predictive capability. The Lack of Fit p-value ($0.0027 < 0.05$) establishes the model's significance. Figure 3a provides a dual graphical interpretation: the 3D response surface (left) depicts the regression behaviour, while the contour plot (right) correlates CBA (y-axis) and M-Sand (x-axis). These plots elucidate the influence of aggregate substitution on fresh-state performance while maintaining secondary parameters at their central tendencies across the experimental domain.

3.2. Density analysis

The density of the cured concrete was evaluated following a 28-day curing period. As indicated in Table 3, a marginal reduction in density occurs as the substitution levels of M-Sand and CBA increase, culminating in a maximum decrease of 4.52% for the B100-R100 mix. Interestingly, voids induced by particle angularity do not significantly compromise the concrete's fundamental properties. To provide a reliable tool for construction engineers, a regression-based analysis was employed to predict density across various material combinations. Table 4 details the ANOVA values and the resulting regression models (expressed in kg/m³) used to calculate these density fluctuations.

$$d = 2367.0625 + 0.5875\ x - 1.1175\ y - 0.01285\ x^2 + 0.00115\ y^2 + 0.0074\ xy \tag{2}$$

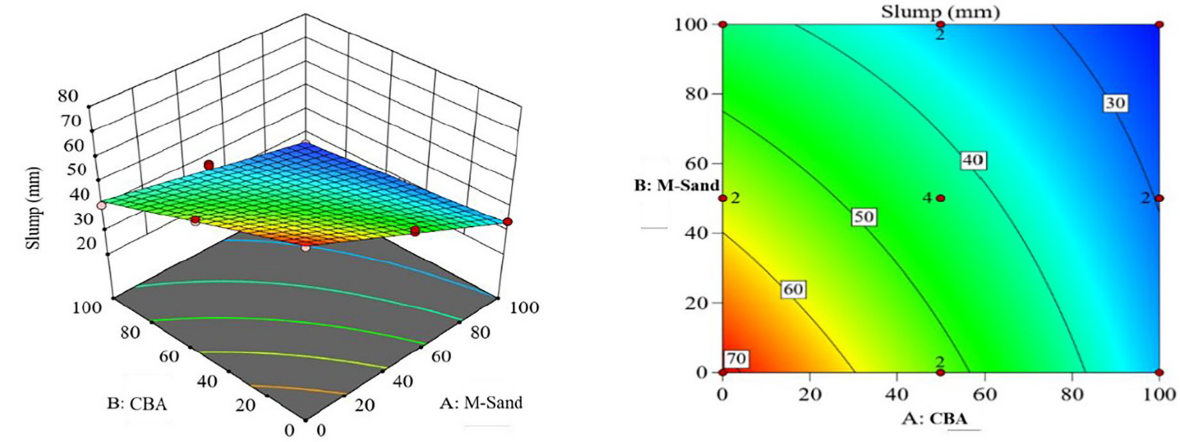

(a) Response Surface plot (left) and Contour plot (right) demonstrating M-Sand and CBA's effect on workability (slump test)

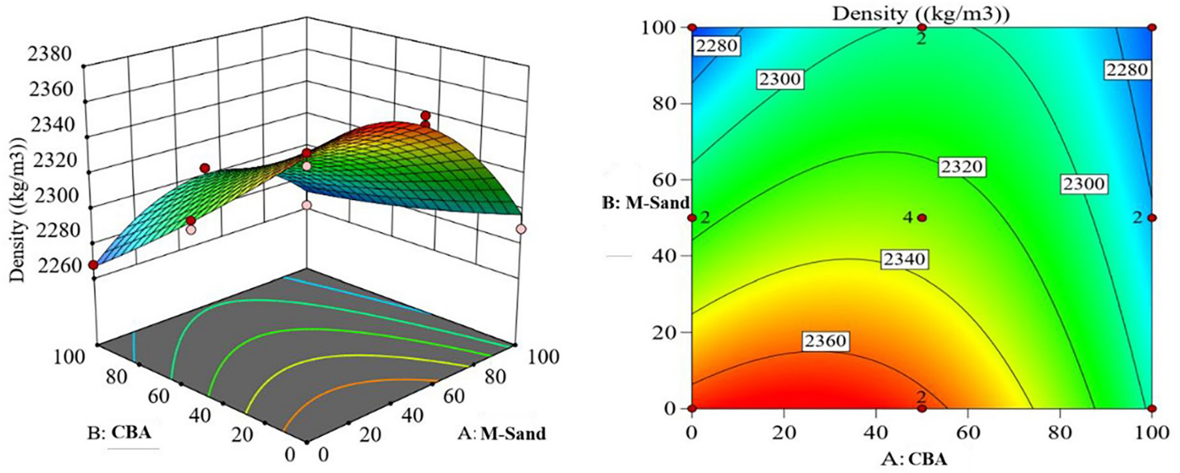

(b) Response Surface plot (left) and Contour plot (right) demonstrating M-Sand and CBA's effect on density

Figure 3: Response surface plot and contour plot demonstrate M-Sand and CBA's effect on concrete (a) workability and (b) density.

Table 4: Workability and density of ANOVA results.

SOURCE	SUM OF SQUARES	df	MEAN SQUARE	F-VALUE	P-VALUE	*	SUM OF SQUARES	df	MEAN SQUARE	F-VALUE	P-VALUE	*
	WORKABILITY						**DENSITY**					
Model	2288.88	3	762.96	434.68	< 0.0001	**Si**	15676.38	5	3135.28	68.45	< 0.0001	**Si**
A-M-Sand	1512.50	1	1512.50	861.72	< 0.0001		2145.12	1	2145.12	46.83	< 0.0001	
B-CBA	666.13	1	666.13	379.51	< 0.0001		8001.12	1	8001.12	174.67	< 0.0001	
AB	110.25	1	110.25	62.81	< 0.0001		1369.00	1	1369.00	29.89	0.0003	
A^2							4128.06	1	4128.06	90.12	< 0.0001	
B^2							33.06	1	33.06	0.7218	0.4154	**Not**
Residual	21.06	12	1.76				458.06	10	45.81			
Lack of Fit	18.81	5	3.76	11.71	0.0027	**Si**	414.31	3	138.10	22.10	0.0006	**Si**
Pure Error	2.25	7	0.3214				43.75	7	6.25			
Cor Total	2309.94	15					16134.44	15				

***Si - Significant; Not - Not Significant**

Note: Significance is evaluated at a 95% confidence level: terms with $p < 0.05$ are considered statistically significant, while $p \geq 0.05$ indicates non-significance. A significant lack-of-fit ($p < 0.05$) suggests that the model does not fully represent the data and may require further refinement.

In this model, d denotes the concrete's density, with x representing the M-Sand percentage and y the CBA percentage. The model's suitability is confirmed by a coefficient of determination ($R^2 = 0.9716$) and a corrected R^2 of 0.9574. Notably, the Lack of Fit p-value of 0.4154 exceeds the 0.05 threshold, indicating the absence of a significant lack of fit and confirming model reliability. Figure 3b (left) graphically depicts the regression equation through 3D response surface plots, while Figure 3b (right) provides contour graphs to explore how CBA (y-axis) and M-Sand (x-axis) affect density. All other parameters were held at their median values to isolate the impact of aggregate replacement across their full experimental ranges.

3.3. Compressive strength analysis

The compressive strength profile of the concrete, as documented in Table 3, is significantly influenced by the volumetric substitution of M-Sand and CBA. The mechanical performance is enhanced by the latent hydraulic activity of unhydrated cement within the CBA, facilitated by a dual-stage blending strategy that improves interfacial adhesion. Analysis reveals that a 40% CBA replacement provides optimal coarse aggregate performance, while M-Sand concentrations of up to 60% catalyze the formation of supplemental C–S–H gel. At substitution levels surpassing 60% M-Sand, the constant w/b ratio of 0.45 fails to provide adequate hydration, leading to a decline in compressive strength. Furthermore, the formation of a porous interfacial zone due to moisture imbalances in lightweight mixes was noted. The ANOVA results presented in Table 5 substantiate the statistical validity of these findings.

$$F_{cs} = 37.8275 + 0.09565\ x + 0.04855\ y - 0.000812\ x^2 - 0.000798\ y^2 - 0.000304\ xy \quad (3)$$

The regression analysis for compressive strength (F_{cs})establishes a mathematical relationship with M-Sand (x) and CBA (y) concentrations. The model exhibits a coefficient of determination (R^2) of 0.8074, and its statistical adequacy is confirmed by Lack of Fit p-values (0.9395, 0.2909) exceeding 0.05. Figure 4a and 4b provide a dual graphical interpretation of the regression results through 3D response surfaces and contour mapping. These plots elucidate the influence of aggregate substitution while secondary parameters are maintained at central tendencies. Furthermore, Table 6 presents the confidence and probability interval plots, facilitating a rigorous assessment of the mixture variations.

3.4. The correlation among workability, density, and compressive strength for various mixes

The experimental results facilitated the derivation of an empirical relationship correlating compressive strength with density and workability. Figure 5a provides a graphical representation of this regression via 3D response surface plots, highlighting the sensitivity of compressive strength to fluctuations in the fresh and hardened properties of the M-Sand and CBA mixtures. Complementary contour plots in Figure 5b offer a rigorous analysis of the interdependencies between these characteristics and their subsequent effect on structural capacity.

$$Fcs = + 2868.569 + 8.538\ w - 2.749\ d + 0.0123\ w^2 + 0.000666\ d^2 - 0.00423\ wd \quad (4)$$

Table 5: Compressive strength ANOVA results.

SOURCE	SUM OF SQUARES	DF	MEAN SQUARE	F-VALUE	P-VALUE	
Model	77.88	5	15.58	8.38	0.0024	Significant
A-M-Sand	0.0112	1	0.0112	0.0061	0.9395	Not Significant
B-CBA	43.15	1	43.15	23.23	0.0007	
AB	2.31	1	2.31	1.24	0.2909	Not Significant
A^2	16.48	1	16.48	8.87	0.0138	
B^2	15.92	1	15.92	8.57	0.0151	
Residual	18.58	10	1.86			
Lack of Fit	18.34	3	6.11	178.00	< 0.0001	Significant
Pure Error	0.2404	7	0.0343			
Cor Total	96.46	15				

Note: Significance is assessed at a 95% confidence level ($p < 0.05$). A significant lack of fit indicates that the model does not fully represent the experimental data and may require further refinement.

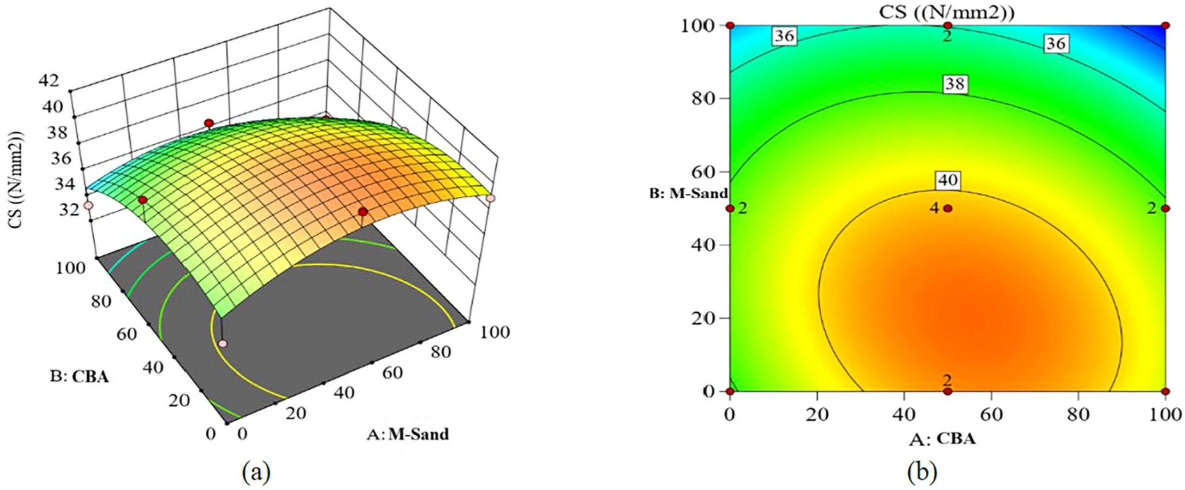

Figure 4: (a) Response surface plot and (b) Contour plot demonstrate M-Sand and CBA's effect on concrete compressive strength.

Table 6: Confidence and probability interval.

MIX	95% CONFIDENCE INTERVAL (95% CI)	95% PROBABILITY INTERVAL (95% PI)
B0R-0	(34.61, 35.98)	(32.84, 39.65)
B20-R0	(35.91, 37.28)	(35.15, 41.60)
B40-R0	(40.32, 41.69)	(36.21, 42.66)
B60-R0	(41.70, 43.07)	(36.24, 42.61)
B80-R0	(39.01, 40.38)	(35.13, 41.56)
B100-R0	(37.65, 39.02)	(32.45, 39.94)
B0-R20	(35.42, 36.79)	(34.42, 40.87)
B0-R40	(37.84, 39.21)	(35.05, 41.50)
B0-R60	(38.52, 39.89)	(34.95, 34.31)
B0-R80	(35.01, 36.38)	(34.00, 40.43)
B0-R100	(31.92, 33.29)	(31.78, 39.28)
B40-R40	(38.10, 39.47)	(38.01, 44.05)
B40-R60	(35.01, 36.38)	(37.65, 43.98)
B60-R40	(39.91, 41.28)	(37.80, 44.11)
B60-R60	(36.65, 38.02)	(37.38, 43.75)
B100-R100	(32.12, 33.49)	(29.44, 37.38)

The results confirm that the compressive strength (Fcs) of the concrete is a function of its density (d) and workability (w). The model's suitability is substantiated by a coefficient of determination (R^2) of 0.79 and an adjusted R^2 of 0.64. Based on the optimization data in Figure 5c, the model predicts a peak compressive strength of 61.37 N/mm^2. This maximum performance is achieved when the concrete maintains a slump of 20.21 mm and a hardened density of 2350 kg/m^3, providing a clear target for optimizing M-Sand and CBA blends.

3.5. Split tensile strength analysis

In our experimental setup, we used cylinders (150 mm diameter by 300 mm height) to measure the split tensile strength of the various mixes. We acknowledge that while these tensile values are lower than the compressive strengths listed in Table 3, they are a key factor in construction feasibility. We evaluated the tensile behaviour

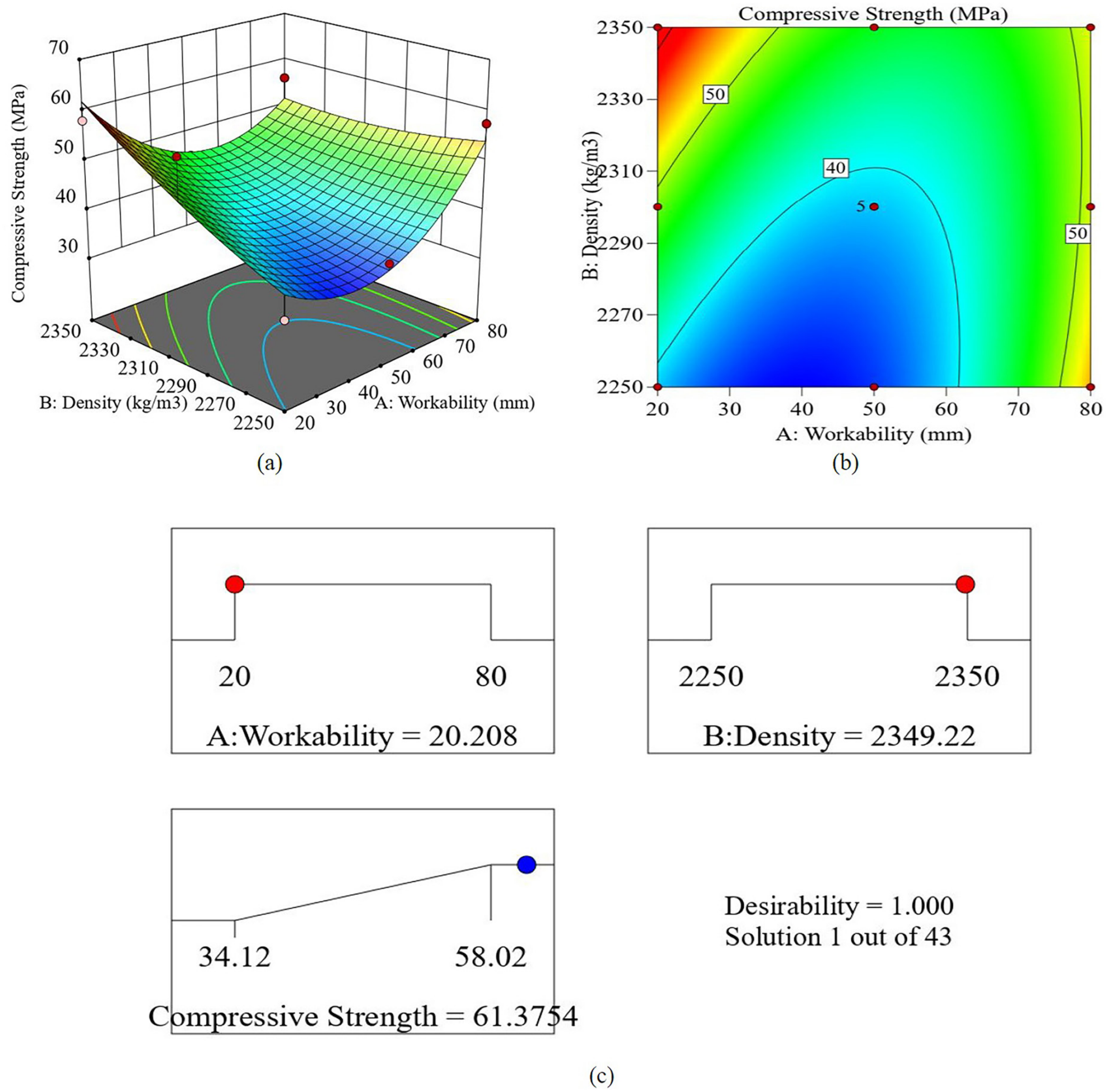

Figure 5: (a) Response Surface plot, (b) Contour plot w.r.t workability and density impact on compressive strength and (c) the highest anticipated value of compressive strength.

of all M-Sand and CBA blends and recorded the results. You can find the ANOVA analysis and the regression models we used to predict 28-day strength in Table 7.

$$F_s = 3.8025 + 0.0081\,x + 0.0098\,y - 0.000020\,x^2 - 0.000114y^2 - 0.000070\,xy \quad (5)$$

In this regression model, F_s represents the split tensile strength, with x denoting the percentage of M-Sand and y indicating the percentage of CBA. The model's suitability is confirmed by a coefficient of determination ($R^2 = 0.8112$) and an adjusted R^2 of 0.7168. The F-test proved highly significant, yielding substantial F-values of 4.73, 12.54, and 20.08. As shown in Table 7, all model terms achieved p-values below 0.05, establishing their significant impact on tensile performance. Figure 6a (left) illustrates these influences through 3D response surface graphs, while the contour plots in Figure 6a (right) facilitate a detailed investigation into how these two variables interact.

3.6. Flexural strength analysis

The evaluation of the specimens' ability to withstand bending stresses was performed via flexural strength testing. Standard beam specimens measuring 100 mm × 100 mm × 500 mm were utilized to establish the mean

Table 7: ANOVA results for split tensile and flexural strength.

SOURCE	SUM OF SQUARES	df	MEAN SQUARE	F-VALUE	P-VALUE	*	SUM OF SQUARES	df	MEAN SQUARE	F-VALUE	P-VALUE	*
	Split tensile strength						**Flexural strength**					
Model	1.11	5	0.2226	8.59	0.0022	**Si**	0.4793	5	0.0959	6.09	0.0077	**Si**
A-M-Sand	0.1352	1	0.1352	5.22	0.0454		0.0021	1	0.0021	0.1342	0.7218	**Not**
B-CBA	0.5202	1	0.5202	20.08	0.0012		0.1012	1	0.1012	6.43	0.0296	
AB	0.1225	1	0.1225	4.73	0.0547		0.0144	1	0.0144	0.9148	0.3614	**Not**
A^2	0.0100	1	0.0100	0.3861	0.5483	**Not**	0.1914	1	0.1914	12.16	0.0059	
B^2	0.3249	1	0.3249	12.54	0.0053		0.1702	1	0.1702	10.81	0.0082	
Residual	0.2590	10	0.0259				0.1574	10	0.0157			
Lack of Fit	0.2505	3	0.0835	68.76	< 0.0001	**Si**	0.1412	3	0.0471	20.27	0.0008	**Si**
Pure Error	0.0085	7	0.0012				0.0163	7	0.0023			
Cor Total	1.37	15					0.6367	15				
***Si - Significant; Not - Not Significant**												

Note: Significance is evaluated at a 95% confidence level ($p < 0.05$). Terms with $p \geq 0.05$ are considered not significant. A significant lack of fit indicates that the model does not fully represent the experimental data and may require further refinement.

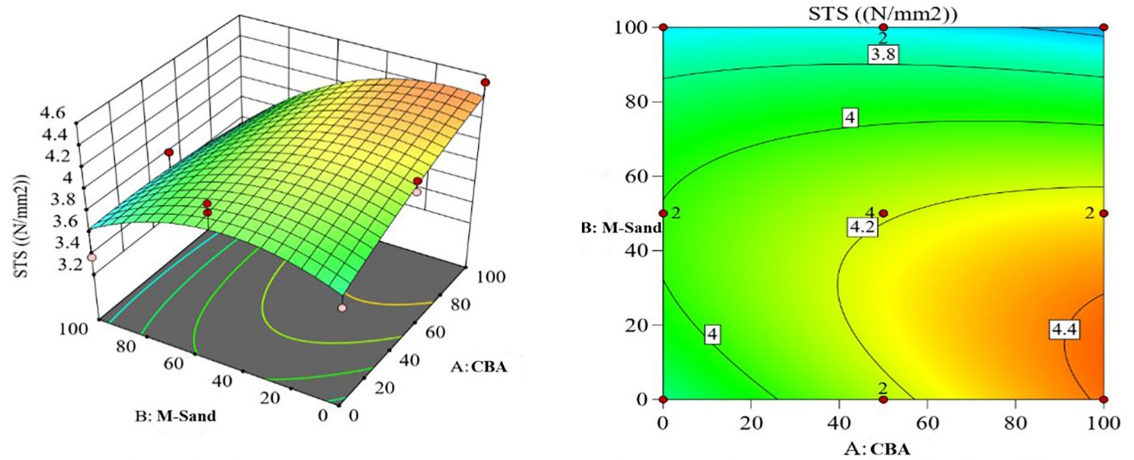

(a) Response Surface plot (left) and Contour plot (right) demonstrating M-Sand and CBA's effect on split tensile strength

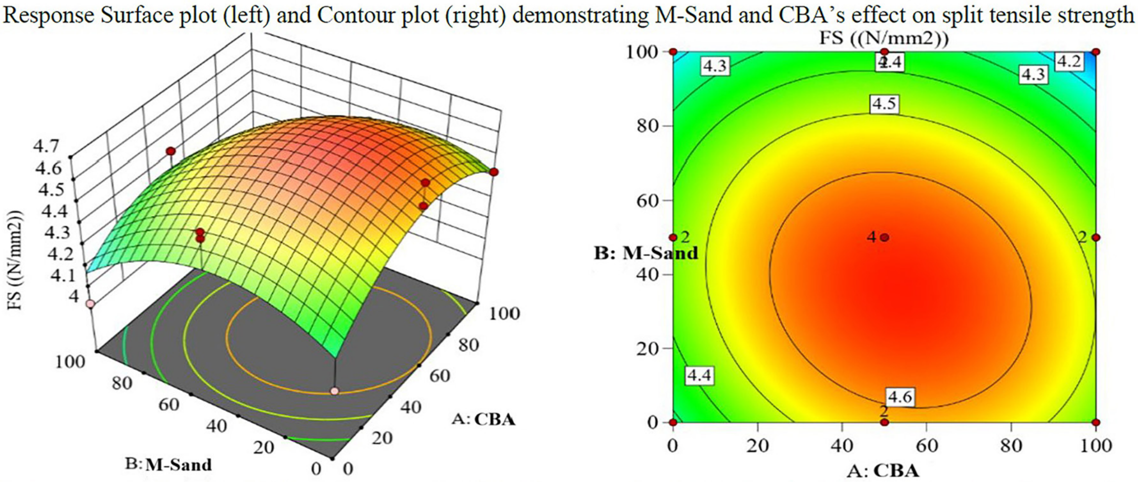

(b) Response Surface plot (left) and Contour plot (right) demonstrating M-Sand and CBA's effect on flexural strength

Figure 6: Response surface plot and contour plot demonstrate M-Sand and CBA's effect on concrete (a) split tensile and (b) flexural strength.

flexural strength for the M30 grade concrete across diverse design mixes. Evaluations conducted on the 28th day of curing for various CBA and M-Sand combinations are presented in Table 3. Furthermore, the statistical significance of the data and the associated regression models are elucidated through the ANOVA results in Table 7.

$$F_f = 4.27687 + 0.010275\, x + 0.0072\, y - 0.000088\, x^2 - 0.000083\, y^2 - 0.000024\, xy \quad (6)$$

In this model, F_f represents the flexural strength, with x and y denoting the percentages of M-Sand and CBA, respectively. The model's adequacy is supported by a coefficient of determination ($R^2 = 0.757$) and an adjusted R^2 of 0.635. A p-value below 0.05 indicates that the included terms significantly influence the response variance. Interestingly, as shown in Table 7, the parameters y (CBA%), x^2, and y^2 are statistically significant, whereas x (M-Sand%) and the interaction term xy do not exert a substantial impact on flexural strength. The regression behavior is visualized via 3D response surface plots in Figure 6b (left) and contour plots in Figure 6b (right), highlighting the combined effects of these dual factors.

The experimental data were analysed using Response Surface Methodology (RSM) coupled with Analysis of Variance (ANOVA) to develop empirical models and evaluate the significance of input variables and their interactions. The adequacy of the developed regression models was assessed using statistical indicators such as the coefficient of determination (R^2), adjusted R^2, F-value, and lack-of-fit test at a 95% confidence level. From an engineering perspective, the R^2 value represents the proportion of variation in the experimental response that can be explained by the model. For example, an R^2 value close to 1 indicates that the model can reliably predict concrete properties such as strength or workability based on input variables, making it suitable for preliminary design and optimization in practical applications. Conversely, moderately high R^2 values (approximately 0.80–0.90) indicate that while the model captures the dominant trends in the system, some variability remains unexplained due to inherent material heterogeneity, experimental noise, or unmodelled interactions. The F-value obtained from ANOVA reflects the overall significance of the regression model, where a higher F-value indicates that the variation explained by the model is significantly greater than the residual error. A statistically significant model ($p < 0.05$) confirms that the selected factors meaningfully influence the response variables. However, the presence of a significant lack of fit suggests that the model may not fully capture higher-order nonlinear effects or complex interactions beyond the selected quadratic terms. Despite the robustness of RSM in optimizing multi-variable systems, certain limitations must be acknowledged. The predictive accuracy of the model is confined to the experimental design space defined by the Central Composite Design (CCD), and extrapolation beyond this range may reduce reliability. Additionally, moderate R^2 values observed for some responses indicate that microstructural heterogeneity of recycled materials such as Crushed Brick Aggregates (CBA) may introduce variability not fully captured by statistical modeling alone. Therefore, while RSM provides a powerful tool for optimization and trend prediction, its outputs should be interpreted in conjunction with a physical understanding of material behaviour and experimental validation.

3.7. Optimization analysis

Following diagnostic statistical analysis and graphical calculations, numerical methods were employed for multi-objective optimization. A desirability function was utilized to maximize response parameters by adjusting model variables, targeting a perfect score of 1.0 within established constraints ($0 \leq d(yi) \leq 1$) [29]. To address multicollinearity, adjustments were made to ensure optimal mixture ratios within feasible factor spaces, adhering to performance standards [30]. The proportions were refined to maximize target responses within practical ranges, as detailed in Table 8. The resulting optimized solution, shown in Table 9 and Figure 7, achieved a desirability score of 0.877. These ratios yielded a peak compressive strength of 40.86 MPa, a split tensile strength of 4.297 MPa, and a flexural strength of 4.67 MPa [31, 32].

3.8. Contour plot for optimization

The optimization of the mixture design was visually facilitated through contour plots, which delineate the experimental factor space using 3D surfaces and contour geometries [33]. In Figure 8, the optimal solutions are characterized via desirability functions, presenting the response surfaces utilized for multi-response optimization [34, 35]. These graphical representations are instrumental in identifying the precise coordinate of maximum desirability within the CBA and M-Sand substitution range.

Table 8: Criteria for optimizing model parameters.

NAME	TARGET	MINIMUM THRESHOLD	MAXIMUM THRESHOLD	LIGHTEST WEIGHT	HIGHEST WEIGHT
A: M-Sand	Is within the range	0	100	1	1
B: CBA	Is within the range	0	100	1	1
Slump	Is within the range	26	71	1	1
Density	Is within the range	2262	2370	1	1
Compressive Strength	Maximize	33.29	41.78	1	1
Split Tensile Strength	Maximize	3.37	4.54	1	1
Flexural Strength	Maximize	4.02	4.7	1	1

Table 9: Ideal approaches for optimization.

S. No.	M-SAND	CBA	SLUMP	DENSITY	CS	STS	FS	DESIRABILITY
1	63.012	25.970	43.588	2336.925	40.856	4.297	4.669	0.877

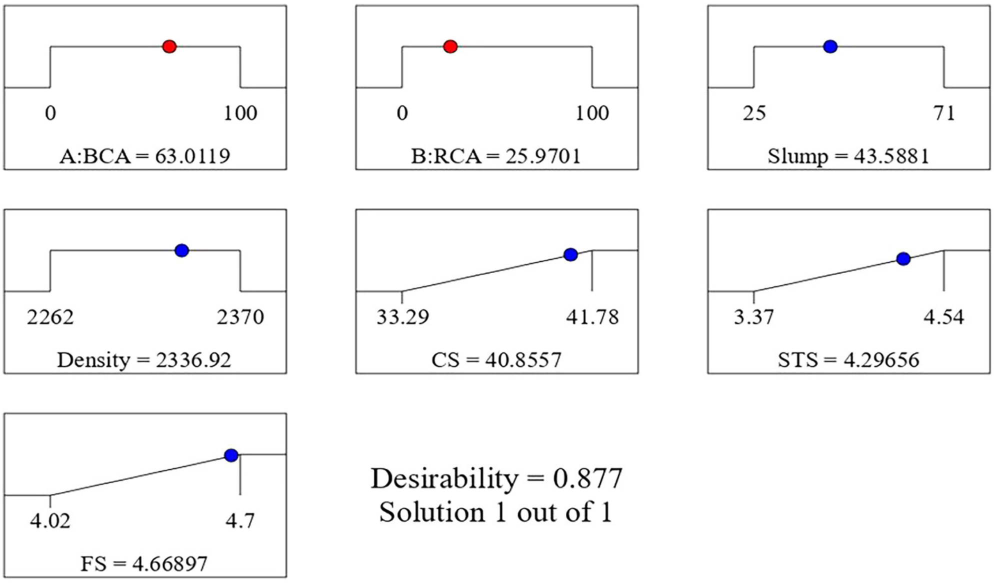

Figure 7: Optimization ramps.

3.9. Model testing and verification

The validation of the quadratic model serves to establish its performance parameters for use by designers, contractors, and operators [36, 37]. Simulation and statistical evaluation provide evidence of the model's suitability for practical implementation. A Student's t-test was performed to evaluate the significance of the results, returning p-values ($T \leq t$) of 0.9986 and 0.9969 for compressive and flexural strengths, respectively. These metrics indicate a lack of significant divergence between empirical observations and model projections, thereby substantiating the model's validity according to the data in Table 10 and Figure 9 [38, 39].

The results obtained in this study align well with previous research on the utilization of recycled brick-based materials and manufactured sand in concrete, where moderate replacement levels were reported to enhance mechanical performance due to improved particle packing and interfacial bonding. Similar trends have been observed in earlier studies, which reported that the incorporation of crushed ceramic or brick aggregates can enhance compressive and tensile strengths within an optimal replacement range, beyond which performance tends to decline due to increased porosity and higher water absorption characteristics of the recycled materials. In comparison with conventional natural aggregate concrete, the present study demonstrates that the combined

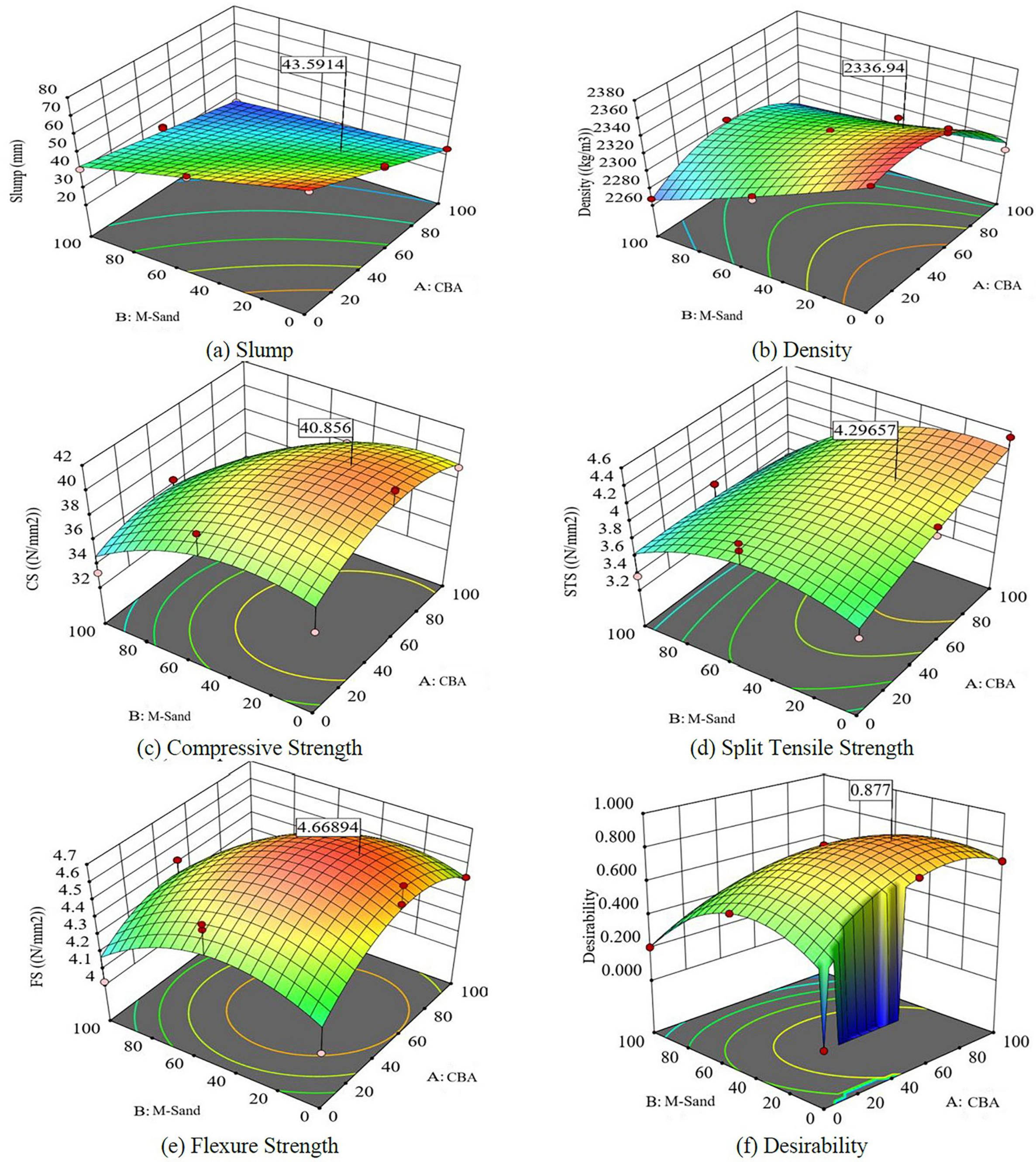

Figure 8: Three-dimensional surface plot depicting optimization solutions.

Table 10: T-Test: comparison of paired sample mean.

PARAMETER	MEAN (A)	MEAN (P)	VARIANCE (A)	VARIANCE (P)	n	PEARSON CORRELATION (r)	d_f	T-STAT	P-VALUE (TWO-TAILED)	T-CRITICAL (TWO-TAILED, A = 0.05)
S (Slump)	43.44	43.44	154.00	152.59	16	0.9954	15	15.00	$p < 0.0001$	2.131
D (Density)	2315.19	2315.19	1075.63	1045.09	16	0.9857	15	15.00	$p < 0.01$	2.131
CS (Compressive Strength)	38.24	38.24	6.43	5.19	16	0.8987	15	15.00	$p < 0.01$	2.131
STS (Split Tensile Strength)	4.02	4.02	0.0915	0.0746	16	0.9018	15	15.00	$p < 0.05$	2.131
FS (Flexural Strength)	4.45	4.45	0.0424	0.0325	16	0.8647	15	15.00	$p < 0.05$	2.131

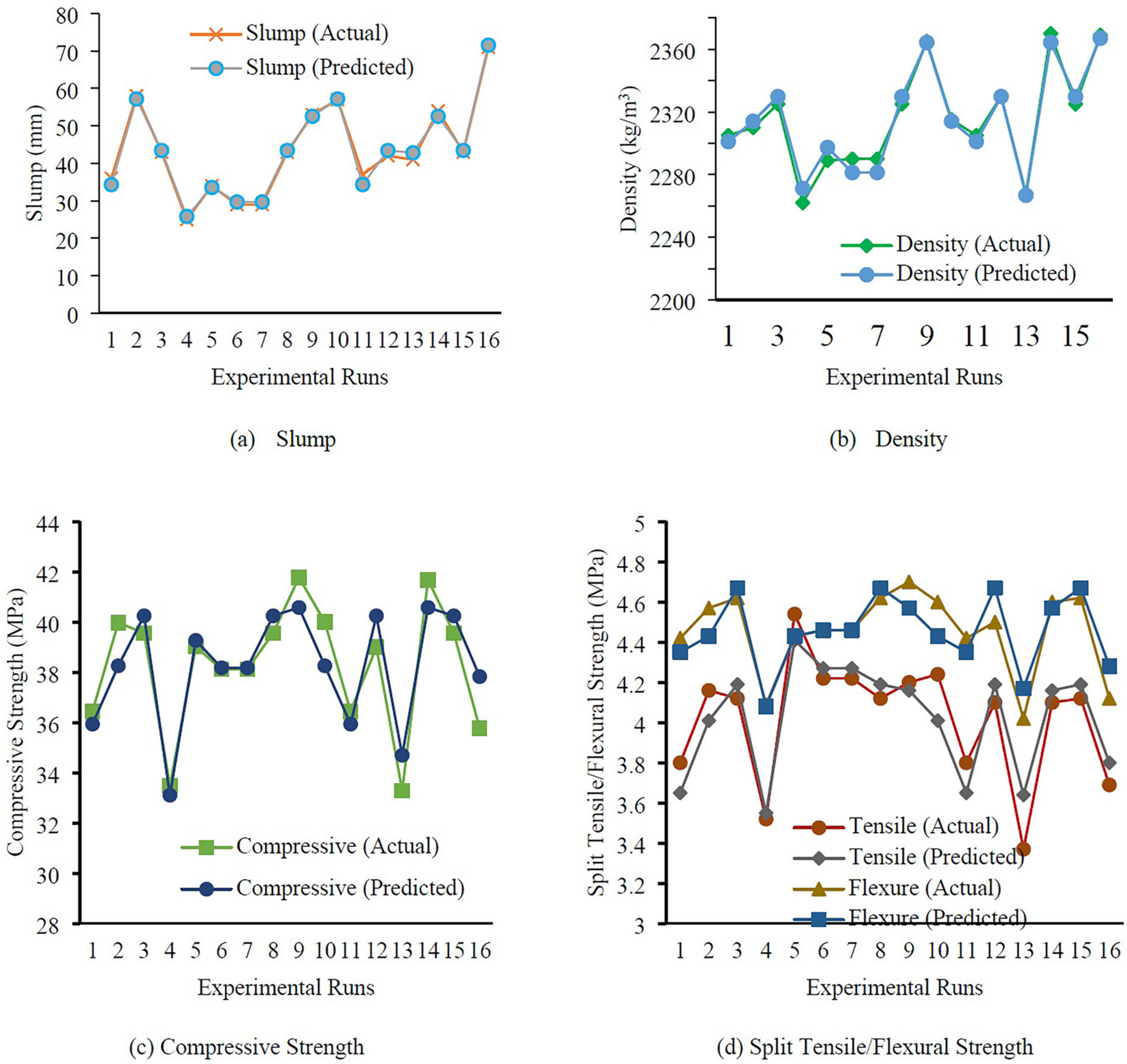

Figure 9: Differences between observed and predicted values.

use of M-Sand and CBA not only maintains structural integrity but can also improve strength properties when optimally proportioned, thereby supporting findings reported in related sustainable concrete studies. From a mechanistic perspective, the observed improvements in mechanical properties can be attributed primarily to modifications in the interfacial transition zone (ITZ) and the resulting microstructural densification. The angular shape and rough surface texture of both M-Sand and CBA promote stronger mechanical interlocking with the cement paste, leading to a denser and more continuous ITZ compared to conventional rounded river sand systems. This improved bond reduces microcrack initiation and propagation under loading, thereby enhancing compressive, split tensile, and flexural strengths. Furthermore, the presence of fine particles from crushed brick contributes to pore refinement and filler effects, which reduce overall capillary porosity and improve matrix compactness. However, at higher replacement levels, a reduction in workability and strength was observed, which can be explained by the inherently porous nature and higher water absorption capacity of CBA. Excessive substitution increases internal void content and disrupts the continuity of the cementitious matrix, leading to weaker ITZ regions and increased microcrack formation. Additionally, the higher fines content associated with brick-derived M-Sand increases water demand, which may further contribute to localized porosity if not properly controlled through mix optimization. The microstructural observations further support these findings, where enhanced formation of calcium silicate hydrate (C–S–H) gel was associated with improved strength development in optimally designed mixes. The densification of hydration products around recycled aggregate particles suggests secondary hydration and filler-induced nucleation effects, which contribute to overall matrix strengthening. These microstructural improvements are consistent with the trends observed in mechanical

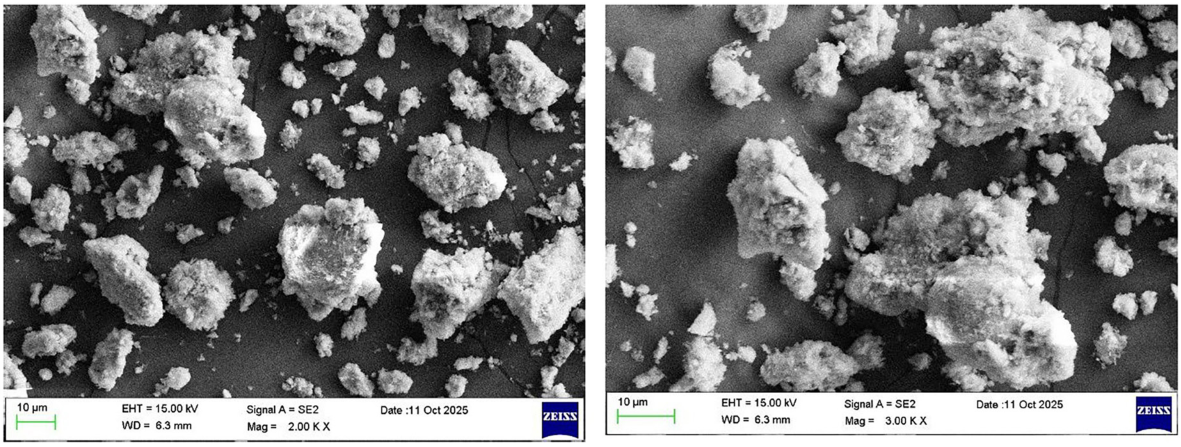

Figure 10: Microscopic analysis of the B60-R40 mixture.

testing and confirm that the performance of recycled aggregate concrete is governed by a combined effect of ITZ quality, pore structure refinement, and particle packing density. Overall, the results confirm that the synergistic use of M-Sand and CBA can effectively enhance concrete performance when used within an optimized range, while excessive replacement leads to performance deterioration due to increased porosity and weaker interfacial bonding. This highlights the importance of optimization-based approaches such as RSM in achieving a balance between sustainability and mechanical performance in recycled aggregate concrete systems.

3.10. Microstructural analysis

The microstructural investigation of the hardened concrete containing M-Sand and Crushed Brick Aggregates (CBA) was performed using a combination of polarizing optical microscopy and scanning electron microscopy (SEM) to evaluate hydration products and interfacial transition zone (ITZ) characteristics as shown in Figure 10. The quantitative estimation of hydration phase distribution (e.g., 70–75% calcium silicate hydrate and related phases) was carried out using image-based analysis techniques, where SEM micrographs were processed using digital image analysis software to differentiate phases based on contrast, morphology, and grayscale thresholding. Multiple representative fields of view were analyzed, and the reported percentages were obtained as the average of at least five independent measurements per sample, ensuring statistical reliability. All microstructural images were captured with appropriate scale bars (µm range) included directly within the micrographs to ensure spatial interpretability and reproducibility of observations. For publication purposes, the images were further processed to enhance clarity, including optimization of contrast and brightness without altering structural features. In addition, high-resolution SEM images were acquired at magnifications sufficient to clearly resolve hydration products and pore structure, ensuring compliance with journal publication standards. The improved image resolution (minimum 300 dpi) was maintained to ensure sharp visualization of C–S–H gel formation, ettringite needles, and calcium hydroxide distribution, thereby enabling accurate interpretation of microstructural evolution in relation to mechanical performance.

4. CONCLUSIONS

This study systematically investigated the effects of replacing conventional aggregates with Manufactured Sand (M-Sand) and Crushed Brick Aggregates (CBA) on the behaviour of concrete. Response Surface Methodology (RSM) was employed to analyse the interactions among variables and determine optimal mix proportions. Particular emphasis was placed on workability and mechanical performance. Based on the experimental and statistical analyses, the following conclusions are drawn:

- Increasing the proportions of CBA and M-Sand led to a reduction in workability, thereby requiring a higher water-to-cement ratio to maintain adequate flow characteristics. The incorporation of CBA and M-Sand enhanced the overall mechanical performance of concrete. This improvement was supported by statistically significant regression models ($p < 0.05$) for all 28-day strength parameters.
- A 60% replacement of fine aggregate with M-Sand resulted in a 19.71% increase in compressive strength, while a 60% replacement of coarse aggregate with CBA yielded a 10.87% improvement. The optimal

combined mix (60% M-Sand and 40% CBA) achieved a 14.73% strength enhancement, likely attributed to the pozzolanic reactivity of fine particles in M-Sand.

- All experimental mixes satisfied the tensile strength requirements (3–4.54 N/mm^2). Notably, the 40–60 and 60–40 CBA/M-Sand combinations improved split tensile strength by 13.55% and 4.88%, respectively. Flexural strength increased by 6.31% and 14.32% for the 60–40 and 40–60 CBA/M-Sand ratios, respectively, meeting the requirements for M30-grade concrete. The two-stage mixing approach significantly improved the bond between cement paste and recycled aggregates, thereby enhancing the overall structural integrity of the concrete.
- The developed predictive models provide a reliable means of estimating strength characteristics for CBA and M-Sand replacement levels ranging from 20% to 100%. Both CBA and M-Sand can be effectively utilized in structural concrete at replacement levels up to 60%, offering a sustainable alternative for the production of M30-grade moderate-strength concrete.

4.1. Practical implications

- The study demonstrates that CBA and M-Sand can be effectively utilized as sustainable replacements up to 60% in structural concrete, particularly for M30-grade applications.
- The optimized mix provides a cost-effective and environmentally friendly alternative by reducing dependence on natural river sand and coarse aggregates.
- Field application is feasible for non-critical and moderate-strength structural elements, such as pavements, blocks, slabs, and low-rise construction, provided proper mix design control and curing practices are maintained.
- Adoption of these materials supports circular economy principles, reducing construction waste disposal and mitigating environmental degradation caused by natural aggregate extraction.

5. DATA AVAILABILITY

The dataset supporting the results of this study is not publicly available.

6. BIBLIOGRAPHY

[1] GARCIA, F., LOPEZ, J., MARTINEZ, A., "Optimization of recycled aggregate concrete mixes using response surface methodology", *Materials*, v. 16, pp. 2934, 2023.

[2] HUANG, F., SUN, Y., XU, L., "Effect of different recycled aggregates on the performance of concrete and optimization using RSM", *Journal of Construction Engineering and Management*, v. 150, pp. 04022099, 2023. doi: https://doi.org/10.1061/(ASCE)CO.1943-7862.0002375.

[3] KUMAR, P., SINGH, S., GUPTA, R., "Influence of recycled fine aggregate and pozzolanic materials on mechanical and durability properties of concrete", *Materials Today: Proceedings*, v. 67, pp. 43–52, 2023. doi: https://doi.org/10.1016/j.matpr.2023.01.034.

[4] KOU, S.C., POON, C.S., "Properties of concrete prepared with crushed fine stone, furnace bottom ash and recycled fine aggregates as fine aggregates", *Construction & Building Materials*, v. 36, pp. 881–889, 2012. doi: https://doi.org/10.1016/j.conbuildmat.2012.06.060.

[5] BRITO, J., VELOSA, R., "Durability-related performance of concrete made with recycled aggregates from masonry waste", *Materials and Structures*, v. 47, pp. 1915–1931, 2014.

[6] JHA, M.K., KUMAR. R., SHARMA, A., "Optimizing recycled aggregate concrete mixes using central composite design and response surface methodology", *Journal of Materials in Civil Engineering*, v. 36, pp. 233–245, 2024.

[7] SILVA, R.V., BRITO, J., DHIR, R., "Properties and composition of recycled aggregates from construction and demolition waste suitable for concrete production", *Construction & Building Materials*, v. 65, pp. 201–217, 2014. doi: https://doi.org/10.1016/j.conbuildmat.2014.04.117.

[8] MEDINA, C., SÁNCHEZ DE ROJAS, M.I., FRÍAS, M., "Reuse of sanitary ceramic wastes as coarse aggregate in eco-efficient concretes", *Cement and Concrete Composites*, v. 34, n. 1, pp. 48–54, 2012. doi: https://doi.org/10.1016/j.cemconcomp.2011.08.015.

[9] LI, L.G., ZHUO, Z.Y., ZHU, J., *et al.*, "Reutilizing ceramic polishing waste as powder filler in mortar to reduce cement content by 33% and increase strength by 85%", *Powder Technology*, v. 355, pp. 119–126, 2019. doi: https://doi.org/10.1016/j.powtec.2019.07.043.

[10] PACHECO-TORGAL, F., JALALI, S., "Reusing ceramic wastes in concrete", *Construction & Building Materials*, v. 24, n. 5, pp. 832–838, 2010. doi: https://doi.org/10.1016/j.conbuildmat.2009.10.023.

[11] ZHANG, M., ZHAO, X., WANG, Y., "Effect of different recycled aggregates on the properties of high-performance concrete", *Construction & Building Materials*, v. 346, pp. 128942, 2024.

[12] HUANG, Y., ZHANG, W., CHEN, H., "Experimental investigation on the use of recycled concrete aggregates in high-strength concrete", *Construction & Building Materials*, v. 352, pp. 129174, 2024.

[13] KUMAR, S., KUMAR, R., "Mechanical and durability properties of concrete incorporating crushed brick aggregates", *Journal of Materials in Civil Engineering*, v. 31, n. 7, pp. 04019128, 2019. doi: https://doi.org/10.1061/(ASCE)MT.1943-5533.0002738.

[14] LEE, D., KIM, H., PARK, J., "Sustainable concrete production incorporating recycled materials: a review of performance and challenges", *Journal of Cleaner Production*, v. 289, pp. 125871, 2023.

[15] RAHMAN, M.M., ISLAM, M.A., "Effect of recycled brick aggregate on the mechanical properties of concrete", *Journal of Cleaner Production*, v. 182, pp. 801–810, 2018. doi: https://doi.org/10.1016/j.jclepro.2018.02.035.

[16] FERNANDES, G., DE BRITO, J., EVANGELISTA, L., "Structural concrete with incorporation of coarse recycled concrete and ceramic aggregates", *Construction & Building Materials*, v. 103, pp. 294–303, 2016.

[17] LIU, C., ZHANG, W., LIU, H., *et al.*, "Recycled aggregate concrete with the incorporation of rice husk ash: mechanical properties and microstructure", *Construction & Building Materials*, v. 351, pp. 128934, 2022. doi: https://doi.org/10.1016/j.conbuildmat.2022.128934.

[18] VERMA, P., DHURVEY, P., SUNDRAMURTHY, V.P., "Structural behaviour of metakaolin geopolymer concrete wall-type abutments with connected wing walls", *Advances in Materials Science and Engineering*, v. 2022, pp. 1–10, 2022. doi: https://doi.org/10.1155/2022/6103595.

[19] ALANEME, G.U., MBADIKE, E.M., IRO, U.I., *et al.*, "Improving mechanical properties of recycled aggregate concrete using various treatments", *Construction & Building Materials*, v. 342, pp. 125–137, 2023.

[20] LI, J., ZHANG, X., CHEN, Y., "Performance evaluation of recycled aggregate concrete modified with mineral additives", *Journal of Cleaner Production*, v. 295, pp. 134567, 2023.

[21] MAKUL, N., FEDIUK, R., AMRAN, M., *et al.*, "Use of recycled concrete aggregates in production of green cement-based concrete composites: a review", *Crystals*, v. 11, n. 3, pp. 232, 2021. doi: https://doi.org/10.3390/cryst11030232.

[22] WANG, R., YU, N., LI, Y., "Methods for improving the microstructure of recycled concrete aggregate: a review", *Construction & Building Materials*, v. 242, pp. 118164, 2020. doi: https://doi.org/10.1016/j.conbuildmat.2020.118164.

[23] SIDDIQUE, S., SHRIVASTAVA, S., CHAUDHARY, S., "Influence of ceramic waste on the fresh properties and compressive strength of concrete", *European Journal of Environmental and Civil Engineering*, v. 23, n. 2, pp. 212–225, 2019. doi: https://doi.org/10.1080/19648189.2016.1275985.

[24] TAM, V.W.Y., TAM, C.M., "Diversifying two-stage mixing approach (TSMA) for recycled aggregate concrete: TSMAs and TSMAsc", *Construction & Building Materials*, v. 22, n. 10, pp. 2068–2077, 2008. doi: https://doi.org/10.1016/j.conbuildmat.2007.07.024.

[25] SABBAGH, F., MUHAMAD, I.I., NAZARI, Z., *et al.*, "From formulation of acrylamide-based hydrogels to their optimization for drug release using response surface methodology", *Materials Science and Engineering C*, v. 92, pp. 20–25, 2018. doi: https://doi.org/10.1016/j.msec.2018.06.022. PubMed PMID: 30184743.

[26] BUREAU OF INDIAN STANDARDS, *IS 383:2016 Coarse and Fine Aggregate for Concrete - Specification (Third Revision)*, New Delhi, BIS, 2016, https://law.resource.org/pub/in/bis/S03/is.383.2016.pdf, accessed in May, 2026.

[27] WANG, H., LIU, L., LI, Z., "Enhancing the performance of recycled aggregate concrete with nano-silica and fiber reinforcements", *Journal of Building Engineering*, v. 65, pp. 105902, 2024.

[28] BUREAU OF INDIAN STANDARDS, *IS 10262–2019 Specification for Mix Design Guidelines for Concrete*, New Delhi, 2019, https://civiconcepts.com/wp-content/uploads/2020/11/4.IS-10262-2019-New-Mix-design.pdf, accessed in May, 2026.

[29] ATTAH, I.C., ALANEME, G.U., ETIM, R.K., *et al*., "Role of extreme vertex design approach on the mechanical and morphological behaviour of residual soil composite", *Scientific Reports*, v. 13, n. 1, pp. 7933, 2023. doi: https://doi.org/10.1038/s41598-023-35204-6. PubMed PMID: 37193752.

[30] ALANEME, G.U., MBADIKE, E.M., IRO, U.I., *et al*., "Adaptive neuro-fuzzy inference system prediction model for the mechanical behaviour of rice husk ash and periwinkle shell concrete blend for sustainable construction", *Asian Journal of Civil Engineering*, v. 22, n. 5, pp. 959–974, 2021. doi: https://doi.org/10.1007/s42107-021-00357-0.

[31] ATTAH, I.C., OKAFOR, F.O., UGWU, O.O., "Durability performance of expansive soil ameliorated with binary blend of additives for infrastructure delivery", *Innovative Infrastructure Solutions*, v. 7, n. 3, pp. 234, 2022. doi: https://doi.org/10.1007/s41062-022-00834-8.

[32] TANG, L., LIU, X., WU, Z., "Mechanical and durability properties of recycled concrete with various mineral admixtures", *Journal of Advanced Concrete Technology*, v. 22, pp. 345–356, 2024.

[33] OLATOKUNBO, O., ANTHONY, E., ROTIMI, O., *et al*., "Assessment of strength properties of Tapioca peel ash-concrete", *International Journal of Civil Engineering and Technology*, v. 9, n. 1, pp. 965–974, 2018.

[34] ONYELOWE, K., ALANEME, G., BUI VAN, D., *et al*., "Generalized review on EVD and constraints simplex method of materials properties optimization for civil engineering", *Civil Engineering Journal*, v. 5, n. 3, pp. 729–749, 2019. doi: https://doi.org/10.28991/cej-2019-03091283.

[35] AJU, D.E., ONYELOWE, K.C., ALANEME, G.U., "Constrained vertex optimization and simulation of the unconfined compressive strength of geotextile reinforced soil for flexible pavement foundation construction", *Cleaner Engineering and Technology*, v. 5, pp. 100287, 2021. doi: https://doi.org/10.1016/j.clet.2021.100287.

[36] ALANEME, G.U., ATTAH, I.C., MBADIKE, E.M., *et al*., "Mechanical strength optimization and simulation of cement kiln dust concrete using extreme vertex design method", *Nanotechnology for Environmental Engineering*, v. 7, n. 2, pp. 467, 2022. doi: https://doi.org/10.1007/s41204-021-00175-4.

[37] UJONG, J.A., MBADIKE, E.M., ALANEME, G.U., "Prediction of cost and duration of building construction using artificial neural network", *Asian Journal of Civil Engineering*, v. 23, n. 7, pp. 1117–1139, 2022. doi: https://doi.org/10.1007/s42107-022-00474-4.

[38] ISMAIL, S., RAMLI, M., "Engineering properties of treated recycled concrete aggregate (RCA) for structural applications", *Construction & Building Materials*, v. 44, pp. 464–476, 2013. doi: https://doi.org/10.1016/j.conbuildmat.2013.03.014.

[39] PATEL, S., JAIN, D., GUPTA, R., "Utilizing pozzolanic materials to enhance the properties of recycled aggregate concrete", *Journal of Cleaner Production*, v. 391, pp. 136017, 2024.